A New Active Contour Model for Medical Image Analysis—Wavelet Vector Flow

Jinyong Cheng, Yihui Liu, Ruixiang Jia, Weiyu Guo

***Abstract*—A new Active Contour Model based on wavelet transform, called Wavelet Vector Flow (WVF), is proposed in this paper. We define wavelet transform vector, which is used to replace the gradient vector in GVF snake model. The WVF snake model improves GVF snake model, because it is robust against noise and inhomogeneity of medical images. Experimental results show image structure boundaries detected by WVF snake model is more accurate than GVF snake model.**

***Index Terms*—Active contours model, Gradient vector flow snake (GVF), Medical image processing, Image segmentation, Wavelet transform**

I. Introduction

In recent years, there has been a great deal of research on segmenting images with deformable models [1]. Active contours, known as "snakes", have been widely studied and applied in medical image analysis. Their applications includes edge detection [2], segmentation of objects [3], shape modeling[4] and motion tracking[5]. Snakes were first introduced in 1987 by Kass [2]. They generally represent an object boundary as a parameter curve or surface. An energy function is associated with the curve, so the problem of finding an object boundary is cast as an energy minimization process. Typically, the curves are affected by both an internal force and external force. A snake can locate object contours well, once an appropriate initialization is done. However, since the energy minimization is carried out locally, the located contours can be trapped by a local minimum. A number of methods have been proposed to improve the snake's performance [6], [7].

Notably, Xu and Prince have proposed a new deformable model called the "gradient vector flow snake" (GVF) [8], [9]. Instead of directly using image gradients as an external force, it uses a spatial diffusion of the gradient of an edge map of the image. GVF snake was proposed to address the traditional snake's problems of short capture range and inability to track at boundary concavity. But GVF still may not be able to capture object contours in some medical image segmentation. Efforts at improving the original GVF snake's performance have been published recently. Yu and Bajaj proposed to compute the GVF using a polar coordinate representation instead of Cartesian coordinates [10]. In this way, the method can perform better than the original GVF snake in the areas of long thin boundary concavities and boundary gaps. But the capture range of this improved GVF does not seem larger than the original method. J.C. Fu, Chai and Wong proposed a wavelet adaptive filter technique to reduce the zigzag noise characteristics of endocardial borders automatically generated by DP [11]. They survey the performance of the wavelet adaptive filter, the snake, and the medial filter in smoothing over the zigzag borders generated by dynamic programming. It indicates the wavelets have strong ability against the image noise.

In this paper, we present a new model of external forces of active contour models, which is called wavelet vector flow (WVF) fields. This new model improves GVF snake based on wavelet analysis. The WVF fields are dense vector fields derived from images by minimizing energy functional in a variation framework. The minimization is achieved by solving a pair of decoupled linear partial differential equations which diffuses the wavelet vectors of a gray-level or binary edge map computed from the image. We call the active contour, which uses the WVF field as its external force, a WVF snake. Particular advantages of the WVF snake over the GVF snake are robust against image noise and the ability to segment the complicated structure of medical images.

II. Active Contour Models

A. Traditional Snake Model

A snake introduced by Kass is an elastic curve, which from an initial state tries to adjust to the most significant features of the scene [2]. It is deformed due to external forces that attract it towards salient features of the image, and internal forces which try to preserve the condition of smoothness in the shape of the curve. A final solution is given by the minimum total energy of the snake, which is the result of the equation

Manuscript received December 18, 2006.

Jinyong Cheng is with the Department of Information science and technology, Shandong Institute of Light Industry, Jinan China. (phone: 86-0531-89631256; fax: 86-0531-89631256; e-mail: cjy@sdili.edu.cn).

Yihui Liu is with the Department of Information science and technology, Shandong Institute of Light Industry, Jinan China. (e-mail: yxl@ sdili.edu.cn).

Ruixiang Jia is with the Department of Information science and technology, Shandong Institute of Light Industry, Jinan China. (e-mail: jiarx@ sdili.edu.cn).

Weiyu Guo is with the Department of Information science and technology, Shandong Institute of Light Industry, Jinan China. (e-mail: gwy@ sdili.edu.cn).

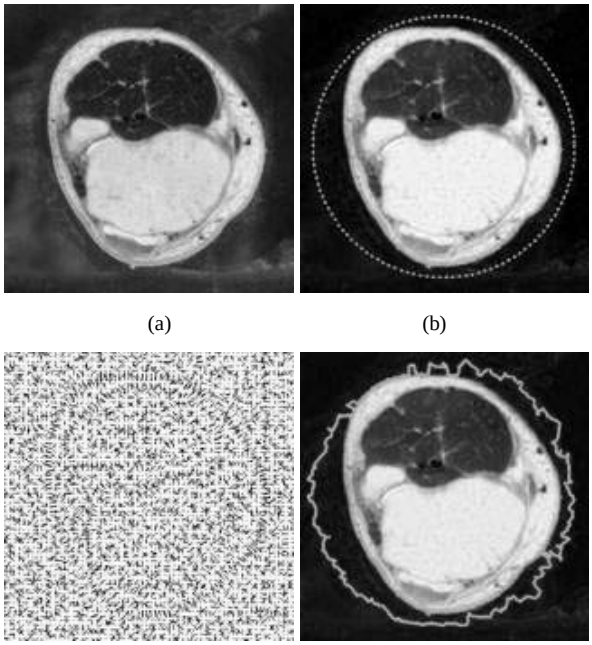

(a) (b)

(c) (d)

Fig.1. An example of border detection (a) medical image slice (b) initial border (c) snake external force field (d) convergence of snake

$$E = \int_0^1 \frac{1}{2}[\alpha \mid X'(s) \mid^2 + \beta \mid X''(s) \mid^2] + E_{\text{ext}}(X(s))ds \qquad (1)$$

Where α and β are weighting parameters that control the snake's tension and rigidity, respectively, $X'(s)$ and $X''(s)$ denote the first and second derivatives of $X(s)$ with respect to *s*. The external energy function E_{ext} is derived from the image so that it takes on its smaller values at the features of interest, such as boundaries.

Given a gray level image $I(x, y)$ which viewed as a function of continuous position variables (x, y) , typical external energies designed to lead an active contour toward step edges are [2]

$$E^1_{\text{ext}}(x, y) = -\mid \nabla I(x, y) \mid^2 \qquad (2)$$

$$E^2_{\text{ext}}(x, y) = -\mid \nabla (G_\sigma(x, y) * I(x, y)) \mid^2 \qquad (3)$$

Where $G_\sigma(x, y)$ is a two-dimensional Gaussian function with standard deviation σ , and ∇ is the gradient operator.

A snake that minimizes *E* must satisfy the Euler equation

$$\alpha X''(s) - \beta X''''(s) - \nabla E_{\text{ext}} = 0 \qquad (4)$$

To find a solution to (4), the snake is made dynamic by treating X as function of time *t* as well as *s* — i.e. $X(s,t)$. Then, the partial derivative of X with respect to *t* is then set equal to the left hand side of (4) as follows

$$X_t(s,t) = \alpha X''(s) - \beta X''''(s,t) - \nabla E_{\text{ext}} \qquad (5)$$

When the solution $X(s,t)$ stabilizes, the term $X_t(s,t)$ vanishes and we achieve a solution of (4). This dynamic equation can also be viewed as a gradient descent algorithm [3] designed to solve (1). A solution to (5) can be found by discretizing the equation and solving the discrete system iteratively.

Although the traditional snake has found many applications, it is intrinsically weak in two main aspects: First, the initial border must be fairly close to the true boundary. Second active contours do not necessarily converge to boundary concavities.

An example of traditional snake applied to a medical slice image is shown in Fig. 1. Fig.1 (a) shows a medical slice image of a human leg. Fig.1 (b) shows the initial border (α =0.6, β =0.0). Fig.1(c) shows the potential force field where pixel. And Fig.1 (d) shows the border output of snake. Because the initial border is far from the true boundary, the active contours can not converge to the true boundary. Clearly, the capture range of traditional snake is very small.

B. GVF (Gradient Vector Flow) Snake Model

Xu and Prince have proposed a new GVF snake to achieve better object segmentation [8]. The GVF snake model remedied both of the shortcomings of the traditional snake. The basic idea of the GVF snake is to extend influence range of image force to a larger area by generating a GVF field. The GVF field is computed from the image. In detail, a GVF field is defined as a vector field $V(x, y) = (u(x, y), v(x, y))$ that minimizes the energy function

$$E = \iint \mu(u_x^2 + u_y^2 + v_x^2 + v_y^2) + \mid \nabla f \mid^2 \mid V - \nabla f \mid^2 \, \mathrm{d}x\mathrm{d}y \qquad (6)$$

Where f is the edge map which is derived by using an edge detector on the original image convoluted with a Gaussian kernel, and μ is a regularization parameter. When $|\nabla f|$ is small, the energy is dominated by the sum of the squares of the partial derivatives of the vector field, resulting a slowly varying yet large coverage field. On the other hand, when $|\nabla f|$ is large, the second term dominates the integral.

Using the calculus of variations, the GVF field can be obtained by solving the following Euler-Lagrange equations

$$\mu\nabla^2 u - (u - f_x)(f_x^2 + f_y^2) = 0 \qquad (7a)$$

$$\mu\nabla^2 v - (v - f_y)(f_x^2 + f_y^2) = 0 \qquad (7b)$$

Where ∇^2 is the Laplacian operator.

Fig.2 shows the result of GVF snake applied to Fig. 1(a). Fig.2 (a) shows the computed GVF field. And Fig.2 (b) shows the border output of GVF snake. In our experiments, we used α =0.6, β =0.0, and μ =0.2 for all GVF. The snakes were dynamically reparameterized to maintain contour point separation to within 0.5–1.5 pixels. In this example of GVF snake, the initial border is same as Fig.1 (b). Comparing the result in Fig.2 (b) to the traditional snake result in Fig.1 (d), we

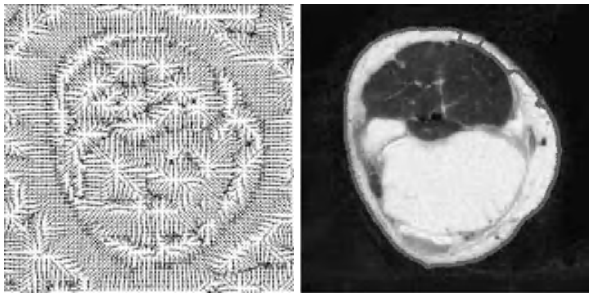

(a) (b)

Fig.2. An example of border detection for GVF snake (a) GVF external force field (b) convergence of GVF Snake

can see that most of the active contours converge to the true boundary. The GVF snake has a much larger capture range than traditional snake. But the GVF snake can not capture right object contours in some medical image. As shown in the top right corner of Fig.2 (b), because of the influence of the image noise, this snake also fails to converge to the true boundary. To deal with these problems, we have developed an improved GVF snake. This new method is presented in detail in the following section.

III. WVF (WAVELETS VECTOR FLOW) SNAKE MODEL

A. Wavelet Analysis

The multi-scale edge detection method based on wavelet transform has been proposed by Mallat [12], [13]. For tow dimensional images, the wavelet transform at scale a contains tow components, W_{a^1} and W_{a^2}, obtained by convolving the image $f(x,y)$ with the wavelets $\psi_{a^1}(x,y)$ and $\psi_{a^2}(x,y)$, respectively

$$W_{a^1} f(x,y) = f(x,y) * \psi_{a^1}(x,y) \tag{8a}$$

$$W_{a^2} f(x,y) = f(x,y) * \psi_{a^2}(x,y) \tag{8b}$$

The wavelets $\psi_{a^1}(x,y)$ and $\psi_{a^2}(x,y)$ are dilations of a mother wavelet which approximates the first derivative of the Gaussian smoothing function $\theta(x,y)$ at scale a.

The two components of the wavelet transform, W_{a^1} and W_{a^2}, represent the gradient vector of the image $f(x,y)$ at scale a. The modulus of the gradient vector is defined as

$$M_a f(x,y) = \sqrt{\left|W_{a^1} f(x,y)\right|^2 + \left|W_{a^2} f(x,y)\right|^2} \tag{9}$$

And the orientation of the gradient vector, $A_a f(x,y)$ is given by

$$A_a f(x,y) = \alpha(x,y) \qquad W_{a^1} f(x,y) \geq 0 \tag{10a}$$

$$A_a f(x,y) = \pi - \alpha(x,y) \quad W_{a^1} f(x,y) < 0 \tag{10b}$$

Where

$$\alpha(x,y) = \tan^{-1}(W_{a^2} f(x,y) / W_{a^1} f(x,y)) \tag{11}$$

B. WVF Snake model

Our overall approach is to define a new external force field, called wavelet vector flow (WVF) field. The main advantage of the WVF field is robust against image noise and ability to segment the complicated medical images.

In the GVF snake model, the vector flow is computed from the gradient vectors of the image. Because gradient operator is sensitive to image noise, the GVF snake performance is not perfect to an image with noise. Wavelet operator has nice anti-noise character. Using multi-scale wavelet transformation, we get the edge image and the wavelet vector. Let the edge image and the vector based on wavelet transform replace the corresponding edge image and the vector in GVF field. Then we define a new snake, which we call the WVF snake.

The gradient of image is a vector contains magnitude $|\nabla f|$ and direction $\arctan(f_y / f_x)$. The vector's magnitude $|\nabla f|$ reflects the step change of the image gray scale, and the vector's direction $\arctan(f_y / f_x)$ reflects the direction of the image edge line [12], [13]. Based on the principle, we define the wavelet transform vector $Wf = (W_{a^1} f(x,y), W_{a^2} f(x,y))$, and let it replace the gradient vector in GVF snake model. From the wavelet transform theory, we can know that besides magnitude and direction, the wavelet transform vector contains two characteristic which wavelet transform is multi-scale and the select of wavelet basis is flexible. When the scale is small, we can get abundant edge detail, but the edge is easily disturbed by the noise. On the other hand, when the scale is large, the edge is steady and the noise reduces, but the precision is fall. Using the multi-scale characteristic of the wavelet analysis, we can get accurate edge and insure nice anti-noise character. Through choosing different wavelet basis, we can receive the best edge-detection effect.

We define the wavelet vector flow (WVF) field to minimize the energy functional

$$E = \iint \mu |\nabla V_w|^2 + |Wf|^2 |V_w - Wf|^2 \, dxdy \tag{12}$$

Where Wf is the vector of wavelet transform with the scale a

$$Wf(a,x,y) = (W_{a^1} f(x,y), W_{a^2} f(x,y)) \tag{13}$$

The following section is an improved algorithm we designed.

1) Through multi-scale edge detection based on wavelet transform to original image, we get the edge image. The choice of the wavelet basis and the largest scale is based on the characters of the target image. For example, to the Fig.1 (a) we can chose the largest scale 3, and chose the

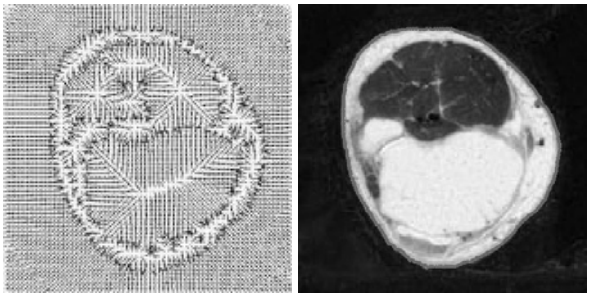

(a) (b)

Fig.3. An example of border detection for WVF snake (a) WVF external force field (b) Convergence of WVF snake

Mexican hat function as the wavelet basis. The filter coefficient is: $h(0) = 0.4317$, $h(1) = 0.2864$, $h(2) = 0.0450$, $h(3) = -0.0393$, $h(4) = -0.0132$, $h(5) = 0.0032$; $g(0) = 0.7118$, $g(1) = -0.2309$, $g(2) = -0.1120$, $g(3) = -0.0226$, $g(4) = 0.0062$, $g(5) = 0.0039$.

2) Perform wavelet transform to the edge image in horizontal direction and vertical orientation, then we get $W_{a^1} f(x,y)$ and $W_{a^2} f(x,y)$. Make $u = W_{a^1} f(x,y)$, $v = W_{a^2} f(x,y)$, and perform iteration management to the edge image with the following formula.

$$u = u + \mu\nabla^2 u - (u - Wf_x)(Wf_x^2 + Wf_y^2) \quad (14a)$$

$$v = v + \mu\nabla^2 v - (v - Wf_y)(Wf_x^2 + Wf_y^2) \quad (14b)$$

After operating it n times, we get the WVF fields. Here, parameter n can be the bigger one in the length and width of the image.

3) Put an initial snake $s = (v_1, v_2, \cdots v_n)$ in the WVF fields, and then let every reference point $v(x,y)$ approach the aim edge by the following formula.

$$x = inv \times (\gamma \times x + \kappa \times wx) \quad (15a)$$

$$y = inv \times (\gamma \times y + \kappa \times wy) \quad (15b)$$

Where wx, wy are vector components of Wf at the reference point. And inv、γ、κ are parameters controlling the approach speed.

Fig.3 shows the result of WVF snake applied to Fig. 1(a). Fig.3 (a) shows the computed WVF field. And Fig.3 (b) shows the border output of WVF snake. Clearly, the WVF snake converges to the boundary more perfectly.

IV. Experiments

Fig.4 shows a few examples that GVF snake and WVF detect the border of medical slice image. Fig.4 (a1)-(a4) show four slices of medical images. Fig.4 (b1)-(b4) show the detection results of GVF snake. Fig.4 (c1)-(c4) show the detection results of WVF snake. To the four slices of images, the detection of the GVF snake departs from the true boundary by the influence of noise. But the WVF snake converges to the true boundary mostly. As shown from the examples, the WVF snake improves the GVF snake model, because it is robust against image noise and segments structure of medical images clearly, which is not easily distinguished due to a small intensity variation.

V. Conclusion

In this paper, we have presented a new method combining Gradient Vector Flow with Wavelet analysis. We define wavelet transform vector, which is used to replace the gradient vector in GVF snake model. We call this improved snake model wavelet vector flow (WVF) snake. Based on experiments on a few slices of medical images, it has shown that the main advantage of the WVF field is its insensitivity to image noise and ability to segment the complicated structure of medical images.

Acknowledgment

The author would like to thank Yanbin Fan, Zhenkuan Pan and Pinglian Song for discussions concerning this work.

References

[1] A. Jain, Y. Zhong, and M. Dubuisson-Jolly, "Deformable template models: A review," Signal Processing, vol. 71, 1998, pp. 109–129.

[2] M. Kass, A. Witkin, D. Terzopouls, "Snake: active contour models," Proceeding of International Journal of Computer Vision, Jan. 1987, pp. 321–331.

[3] D. Terzopoulos, K. Fleischer, "Deformable models," The Visual Computer, Apr. 1988, pp. 306–331.

[4] F. Leymarie, M. D. Levine, "Tracking deformable objects in the plane using an active contour model," *IEEE Transl. on PAMI*, vol. 15, Jun. 1993, pp. 617–634.

[5] D. Terzopoulos, R. Szeliski, "Tracking with Kalman snakes," Artificial Intelligence, USA: MIT Press, 1992, pp. 3–20.

[6] L. D. Cohen, I. Cohen, "Finite-element methods for active contour models and balloons for 2-D and 3-D images," *IEEE Transl. on Patt. Anal. Mach. Intell.*, vol. 15, 1993, pp. 1131–1147.

[7] D. J. Williams, M. Shah, "A fast algorithm for active contours and curvature estimation," CVGIP: Image Understanding, vol. 55, Jan. 1991, pp. 14–26.

[8] C. Xu, J. Prince, "Generalized gradient vector flow external forces for active contours," Signal Processing. vol. 71, 1998, pp. 131–139.

[9] C. Xu, J. Prince, "Snakes, shapes, and gradient vector flow," *IEEE Transl. on Images Processing*, vol. 7, 1998, pp. 359–369.

[10] Z. Yu, C. Bajaj, "Image Segmentation Using Gradient Vector Diffusion and Region Merging," In Proceedings of International Conference on Image Processing, Quebec City, Sep. 2002, pp. 828–831.

[11] J. C. Fu, J. W. Chai, and S. T. C. Wong, "De-noising of left ventricular myocardial borders in magnetic resonance images," Magnetic Resonance Imaging, vol. 20, 2002, pp. 649–657.

[12] S. Mallat, S. Zhang, "Characterization of signals from multiscale edge," *IEEE Transl. PAMI.*, vol. 14, 1992, pp. 710–732.

[13] S. Mallat, W. Hwang, "Singularity Detection and processing with Wavelet," *IEEE Transl. on Information Theory.*, vol. 38, 1992, pp. 617–643.

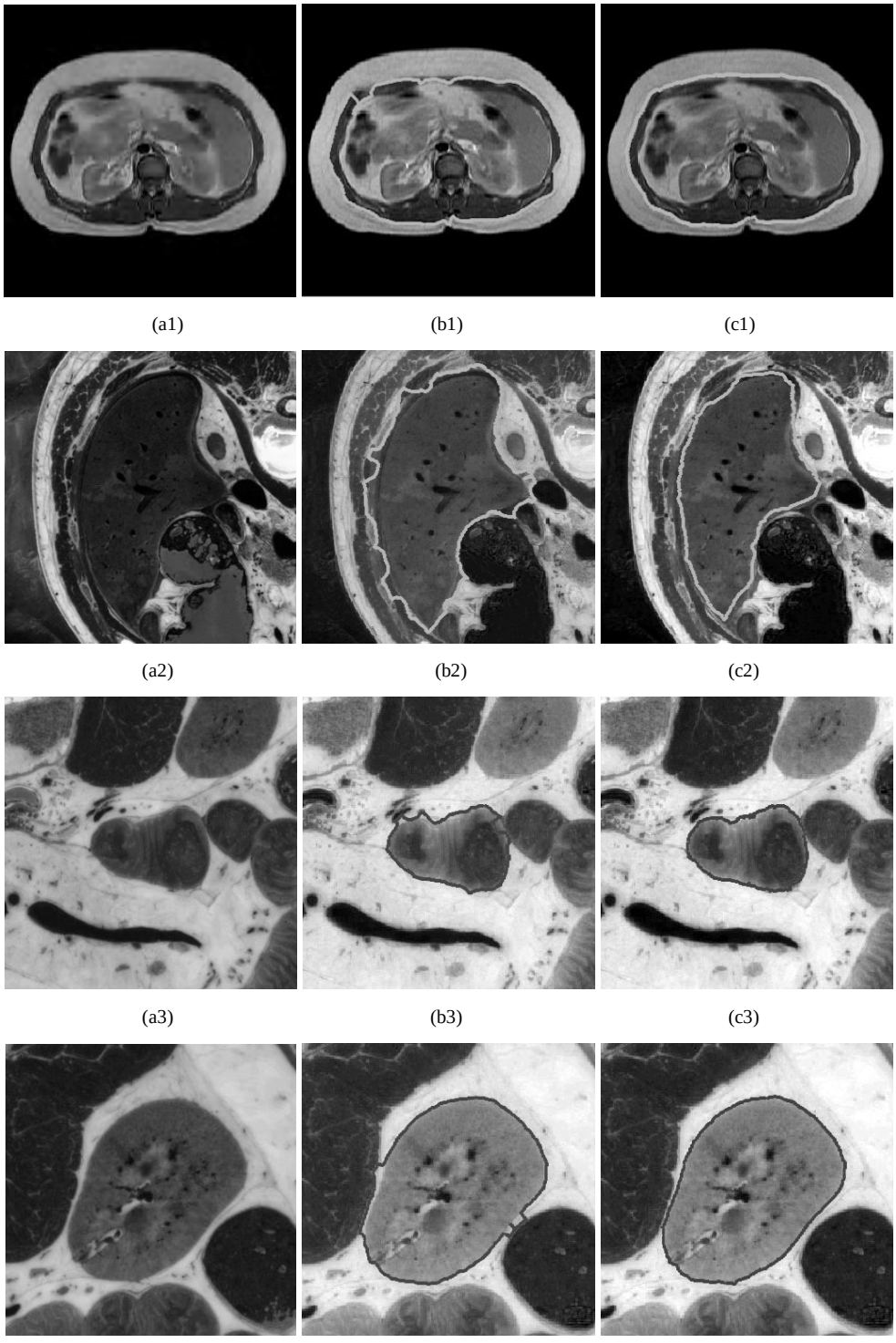

(a1) (b1) (c1)

(a2) (b2) (c2)

(a3) (b3) (c3)

(a4) (b4) (c4)

Fig.4. Examples of edge detection for GVF snake and WVF snake (a1), (a2), (a3) and (a4) slice of medical image (b1), (b2), (b3) and (b4) detection boundary of GVF snake (c1), (c2), (c3) and (c4) detection boundary of WVF snake.